

Structure of Radical Cations of Saturated Heterocyclic Compounds with Two Heteroatoms As Studied by Electron Paramagnetic Resonance, Electron–Nuclear Double Resonance, and Density Functional Theory Calculations

Kirill B. Nuzhdin,^{*,†} Sergej V. Nesterov,[‡] Daniil A. Tyurin,[†] Vladimir I. Feldman,^{†,‡,§,||}
Liu Wei,[⊥] and Anders Lund[⊥]

Department of Chemistry, Moscow State University, 119992 Moscow Russia, Institute of Synthetic Polymeric Materials, The Russian Academy of Sciences, 70 Profsoyuznaya Str., Moscow 117393, Russia, Karpov Institute of Physical Chemistry, 10 Vorontsovo Pole Str., Moscow 105064 Russia, and Department of Physics and Measurement Technology, Linköping University, S-58183, Linköping, Sweden

Received: March 19, 2005; In Final Form: May 19, 2005

The radical cations of piperazine, morpholine, thiomorpholine, and thioxane were investigated by electron paramagnetic resonance (EPR) and electron–nuclear double resonance (ENDOR) spectroscopy in a solid Freon matrix. Optimized geometry and magnetic parameters of the radical cations were calculated using a density functional theory (DFT)/Perdew–Burke–Ernzerhof (PBE) method. Both experimental and theoretical results suggest that all the studied species adopt chair (or distorted chair) conformations. No evidence for the boat conformers with intramolecular σ^* -bonding between heteroatoms were obtained. In the cases of morpholine and thioxane, the oxygen atoms are characterized by relatively small spin populations, whereas a major part of spin density is located at N and S atoms, respectively. The thiomorpholine radical cation exhibits nearly equal spin population of N and S atoms. In most cases (except for thioxane), the calculated magnetic parameters agree with the experimental data reasonably well.

Introduction

In the past 25 years, organic radical cations have been studied extensively by electron paramagnetic resonance (EPR) spectroscopy in low-temperature matrixes.^{1–4} These studies revealed the electronic and geometrical structure of a wide variety of these highly reactive species and provided direct insight into a number of problems of general chemical interest. In particular, radical cations of the six-member heterocycles with two heteroatoms present a simple model for investigation of the effects of spin and charge delocalization and importance of “through-space” interactions in conformationally flexible systems. Furthermore, the knowledge on the structure of such species is of potential interest for understanding the properties of more complex related ionized molecules of biological significance.

In the case of radical cations of saturated heterocyclic compounds containing an O, N, or S atom, the single occupied molecular orbital (SOMO) is definitely associated with the heteroatom.^{1,2} Meanwhile, introduction of a second heteroatom into a saturated ring has a dramatic effect on the SOMO nature. If the heteroatoms are separated by only one methylene group, the effect of “p– σ –p delocalization” results in extraordinarily large hyperfine coupling for “bridge” methylene protons, as was demonstrated for 1,3-dioxo compounds.⁵ On the other hand, for symmetrically substituted six-member 1,4-diheterocycles the situation is not so clear. Among these species, the radical cations

of 1,4-dioxane and 1,4-dithiane were studied in detail. The former radical cation is characterized by relatively small and comparable hyperfine coupling constants for all the eight protons (0.8–1.1 mT).^{2,6–8} In earlier papers, these results were explained either by O–O intramolecular σ^* -bonding occurring in the “boat” structure⁶ or by nearly planar structure.⁷ However, more recent theoretical calculations suggest that the static “chair” conformation may account well for the experimental findings.^{2,8} In contrast, the EPR spectrum of the 1,4-dithiane radical cation was assigned unambiguously to the “boat” structure with a three-electron intramolecular σ^* -bonding.^{9,10} Weak intramolecular bonding was also assumed for a *N,N'*-dimethylpiperazine radical cation;¹¹ however, this interpretation was not tested from a calculational viewpoint. To our knowledge, the six-member heterocyclic radical cations with two different heteroatoms have not yet been characterized experimentally and theoretically (formation of morpholine radical cation in a Freon-113 matrix was mentioned by Antzutkin et al.,¹² but the spectral assignment was not made because the cited paper was focused on secondary radical species).

In this paper, we present the results of experimental and theoretical studies of the radical cations of piperazine, morpholine, thiomorpholine, and 1,4-thioxane (Figure 1, calculated bond lengths in Table 1). These species were generated by irradiation of frozen solutions using a well-known “Freon matrix technique” based on trapping of radiolytically produced radical cation in the fluorinated matrixes with high ionization potential and high electron affinity.^{1–3} In this work, we used Freon-11 (CFCl₃) as a matrix. This polycrystalline medium does not allow any diffusion-induced bimolecular reactions (unlike glassy matrixes, e.g., Freon-113), which makes it possible to observe the primary radical cations up to 155 K.² As the radical cations of the type

* Corresponding author. E-mail: kirill.nuzhdin@rad.chem.msu.ru.

† Moscow State University.

‡ The Russian Academy of Sciences.

§ Karpov Institute of Physical Chemistry.

|| E-mail: feldman@cc.nifhi.ac.ru. Fax: +7 095 4202229. Tel: +7 095 917430.

⊥ Linköping University.

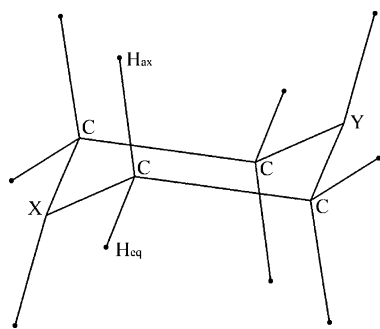


Figure 1. Calculated structure of the radical cation of piperazine ($X = Y = N$). Two hydrogen atoms in axial and equatorial positions are marked as H_{ax} and H_{eq} , respectively. Similar-type structures were found theoretically for other heterocycles ($X = N$, $Y = O$ for morpholine; $X = N$, $Y = S$ for thiomorpholine; $X = O$, $Y = S$ for thioxane). α -Hydrogen atoms are absent, if X , $Y = O$ or S .

TABLE 1: Calculated Bond Lengths for the Radical Cations of Studied Heterocycles

radical cation	C–C bond length	X–C bond length	X–H bond length
piperazine	1.614	1.422 (C–N)	1.096 (C– H_c)
			1.098 (C– H_a)
			1.019 (N–H)
morpholine	1.599	1.403 (C–O) 1.422 (C–N)	1.096 (C_α –O– H_c)
			1.101 (C_α –O– H_a)
			1.095 (C_α –N– H_c)
			1.098 (C_α –N– H_a)
			1.021 (N–H)
thiomorpholine	1.588	1.805 (C–S) 1.427 (C–N)	1.097 (C_α –S– H_c)
			1.097 (C_α –S– H_a)
			1.098 (C_α –N– H_c)
			1.097 (C_α –N– H_a)
			1.020 (N–H)
thioxane	1.575	1.803 (C–S) 1.408 (C–O)	1.097 (C_α –S– H_c)
			1.097 (C_α –S– H_a)
			1.098 (C_α –O– H_c)
			1.100 (C_α –O– H_a)

under consideration often exhibit complicated and poorly resolved EPR spectra with relatively small hyperfine splittings, the electron–nuclear double resonance (ENDOR) technique was used as a complementary tool. Density functional theory (DFT) calculations were carried out to get the theoretical geometry and magnetic resonance parameters of the radical cations. The main goals of this work were (1) to investigate the effect of heteroatoms nature on conformation and electronic structure of 1,4-diheterocyclic radical cations and (2) to make systematic comparison of the DFT predictions with experimental findings for the systems of this kind.

Experimental and Calculation Methods

Piperazine (98%, Merck), morpholine (98%, Reakhim, Russia), thiomorpholine (98%, Aldrich), 1,4-thioxane (98%, Aldrich), and Freon-11 ($CFCl_3$, 99.99%, Khimprom, Volgograd, Russia) were used as received. The solutions of heterocyclic compounds in Freon (0.1–0.5%) were degassed through a standard freeze–pump–thaw cyclic procedure (typically, three cycles) and irradiated with X-rays (Philips X-ray generator) or ^{60}Co γ -rays (K-120000 apparatus) at 77 K. The total absorbed dose was 6–15 kGy. EPR spectra were measured at 77–155 K with a X-band (9.4 GHz) spectrometer with a 100-kHz high-frequency modulation manufactured by SPIN (St. Petersburg, Russia). In the case of combined EPR/ENDOR studies, the EPR and ENDOR spectra were measured at 30–120 K with a Bruker ER200D-SRC CW EPR/ENDOR spectrometer.

Isotropic simulations of the EPR spectra were made with a PEST Winsim software, and anisotropic powder simulations

were carried out with WINEPR Simfonia (Bruker). It is worthwhile noting that the β -proton coupling for all the studied species is expected to be nearly isotropic. Anisotropic contributions are essential for N and α -proton (N–H) couplings in piperazine, morpholine, and thiomorpholine radical cations. In principle, the HFC tensor components could be determined from best-fit powder simulations of the spectra recorded at low temperatures. However, poor spectral resolution at low temperatures and a large number of adjustable parameters make such fitting rather unreliable. Also, ENDOR was found to be not very helpful in this case, because of broadening of anisotropic components and poor signal-to-noise ratio (see below). For this reason, we did not make any speculations on the HFC tensor components. Instead of this, we used best-fit isotropic simulation to determine the isotropic HFC constants from the EPR spectra measured at the highest attainable temperature (typically, 150–155 K), when anisotropic contributions are nearly canceled because of dynamic averaging (see also discussion below).

As mentioned above, ENDOR may be very helpful in the case of poorly resolved EPR spectra resulting from occurrence of a number of relatively small and close in magnitude hyperfine couplings. However, the signal-to-noise ratio in ENDOR is much poorer than that in EPR, so in many cases we were able to get ENDOR signals of appropriate quality only at low temperatures. Basically, the ENDOR spectra exhibit pairs of lines for each set of equivalent magnetic nuclei:

$$\nu_{1,2} = |\nu_H \pm a_H/2|$$

where ν_H is the proton Larmor frequency at the selected magnetic field and a_H is the effective hyperfine coupling of the proton. Meanwhile, one should keep in mind the so-called hyperfine enhancement effect.¹³ Simplifying the formula for the square of the transition moment one can get¹⁴

$$W^2 = (I(I+1) - m_I(m_I \pm 1))(g_N \beta_N B_2)^2 [1 - M_S A_i / \nu_N]^2 / 4$$

where g_N is the nuclear g -factor, A_i is the i -component of the hyperfine tensor that is parallel to the magnetic field, ν_N is the Larmor frequency of the nucleus, B_2 is the RF-field, M_S and m_I are spin and nuclear magnetic moments. The enhancement factor $1 - M_S A_i / \nu_N$ is M_S -dependent and ENDOR transitions for the two M_S -values will in general have different intensities. In the extreme case, the square of the transition moment with $M_S = 1/2$ will be close to zero (if A_i is positive, as it is typical for β -protons), so only the high-field signal could be observed. It is easy to see that the intensity ratio for the low and high-frequency signals will be less than $1/3$ if A_i is between 0.5 and 2.0 mT. This is rather typical, and in our spectra we normally can observe only one line for each pair, which was treated as a high-frequency component. If the hyperfine coupling constants derived from ENDOR data were out of this range, both possible interpretations were considered. Anyway, in most cases, all the observed ENDOR signals were rather weak and noisy. For this reason, we used fitting of the EPR spectrum as the main criterion.

The method of density functional theory (DFT) with the Perdew–Burke–Ernzerhof (PBE) exchange–correlation functional was used for calculations.¹⁵ All DFT calculations were performed using the PRIRODA program^{16,17} with large orbital basis sets of contracted Gaussian-type functions of the size (5s1p):[3s1p] for H, (11s6p2d):[4s3p2d] for C, (11s6p2d):[4s3p2d] for N, (11s6p2d):[4s3p2d] for O, and (16s12p2d):[5s4p2d] for S. The convergence criterion for the geometry

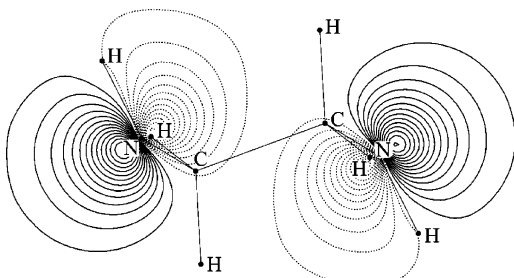


Figure 2. Spin density distribution for the radical cation of piperazine in the N–H bonds plane.

optimizations was set to 1×10^{-7} au for the norm of the gradient, and within each SCF cycle the convergence criterion was 1×10^{-9} au. Energy minima of the optimized molecules have been verified by a calculation of the Hessian. Hyperfine couplings were obtained through spin density at the nuclei with formula¹⁸

$$a_{\text{nuc}}^{\text{iso}} = \frac{4\pi}{3} g_{\text{e}} \beta_{\text{e}} g_{\text{nuc}} \beta_{\text{nuc}} \langle S_z \rangle^{-1} \rho_{\text{nuc}}^{\alpha-\beta}(\delta(r_{\text{nuc}}))$$

Principal values of hyperfine coupling tensor were obtained through principal values of electric field gradient tensor at the nuclei with formula¹⁸

$$T_{\text{nuc}}(i) = \frac{1}{2} g_{\text{e}} \beta_{\text{e}} g_{\text{nuc}} \beta_{\text{nuc}} \langle S_z \rangle^{-1} E(i)$$

Results of Quantum Chemical Calculations

Piperazine. According to calculations, neutral molecule of piperazine in “chair” conformation is over 6 kcal/mol lower in energy than “twist” and “boat”. In turn, the two chair conformations (formed by nitrogen atom inversion) differ by almost 2 kcal/mol (conformation with equatorial N–H bonds position is the lowest one).

Calculation of the radical cations shows that the most favorable conformation is “chair” with N–H bonds taking the axial positions. Calculated spin density distribution (Figure 2) corresponds to eight comparable hyperfine coupling constants for the C–H protons: $a_1(4\text{H}) = 0.68$ and $a_2(4\text{H}) = 0.88$ mT (see Table 2). Obviously, the hyperfine couplings of unpaired electron with nitrogen and α -hydrogen (adjacent to N) atoms exhibit remarkable anisotropy. Regarding the calculated isotropic hyperfine coupling (HFC) constant for the ¹⁴N nucleus, we may note that this value is probably somewhat underestimated (this effect was revealed in the test calculation of known amine radical cations using the same method). Principal values of anisotropic hyperfine tensors are also given in Table 2. It makes sense to take into account anisotropic hyperfine tensors only for nitrogen atoms and α -protons because of their considerably large values.

According to our calculations, the energy of distorted “boat” conformation with axial and equatorial N–H bond positions are essentially less stable than the “chair” conformer (by 9.3 and 12.4 kcal/mol, respectively). One of the calculation results we have is that for the boat conformers one should expect a number of large proton hyperfine coupling constants (from 1.9 up to 5.0 mT).

Morpholine. According to calculations, the most favorable conformation for a neutral morpholine molecule is “chair” (N–H bond in equatorial position). The energy of other calculated conformers, “twist” and “boat” (two conformations with axial and equatorial N–H bond positions) is, at least, 6 kcal/mol higher. Two conformations were found in calculations

TABLE 2: Comparison of Experimental and Calculated Hyperfine Coupling Constants for the Radical Cations of Studied Heterocycles

radical cation	atom	calcd isotropic constants, mT ^a	exptl constants (EPR/ENDOR), mT ^{b,c}
piperazine	2N	0.74 (0.14; 0.14; 1.94)	(0.95)
	2H _α	0.76 (0.04; 0.63; 1.61)	(1.15)
	4H _β –N (1)	0.89	(0.96)
	4H _β –N (2)	0.68	(0.91)
morpholine	N	0.75 (–0.09; –0.09; 2.43)	(1.11)
	H _α	1.16 (0.17; 0.97; 2.34)	(1.47)
	2H _β –O	0.44	0.45
	2H _β –O	0.83	0.90
	2H _β –N	0.52	0.52
thiomorpholine	2H _β –N	1.48	(1.66)
	N	0.77 (0.11 0.11 2.09)	(1.05)
	H _α	0.86 (0.08 0.71 1.79)	(1.37)
	2H _β –S	0.12	0.24
	2H _β –N	0.77	1.01
thioxane	2H _β –S	0.82	1.18
	2H _β –N	0.93	1.61
	2H _β –S	0.02	0.57
	2H _β –O	0.34	0.77
	2H _β –O	0.93	2.13
	2H _β –S	1.42	2.32

^a The principal values of the hyperfine coupling tensor for N and α -H nuclei are given in parentheses. ^b The values determined from fitting of simulated EPR spectra are given in italics in parentheses. ^c Accuracy of direct determination of the HFC constants from experimental spectra is limited by relatively large line width (uncertainty of, at least, 0.1 mT). Meanwhile, the simulated spectra are sensitive to variations of these parameters by more than ± 0.03 mT, which affect the total spread of the spectra, especially, in the case of large number of interacting protons.

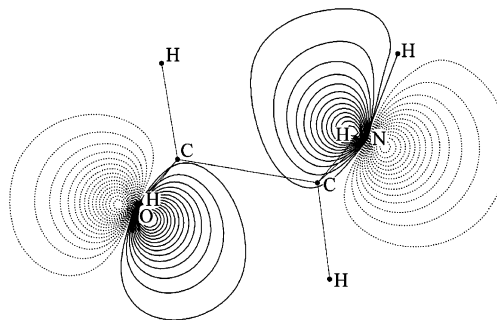


Figure 3. Calculated spin density distribution for the radical cation of morpholine in the N–H bond–oxygen atom plane.

for the morpholine radical cation: “chair” and “boat” with the axial position of N–H bond. The former conformation is definitely more stable (calculated energy difference is 8.76 kcal/mol). In the case of “chair” conformation, the spin density is mostly located at the P_z orbital of the nitrogen atom (Figure 3), and the largest hyperfine splitting in the EPR spectrum should be observed from the two corresponding β -hydrogen atoms (1.48 mT). The two hydrogen atoms (in the β -position with respect to the oxygen atom) reveal the hyperfine coupling constant of 0.83 mT. Other calculated hyperfine coupling constants are quite small (see Table 2).

In the case of “boat” conformation, the spin population on the nitrogen atom is larger than that for the “chair” conformation case. Therefore, one could expect the occurrence of two protons characterized by large hyperfine coupling constants (according to our calculations, above 2.5 mT).

Thiomorpholine. In the case of the neutral thiomorpholine molecule, the calculation shows two conformations with very close energies, namely, “chair” conformations with axial and equatorial N–H bond positions, respectively. Other calculated minima corresponding to distorted “boat” conformations lie, at least, 7 kcal/mol above.

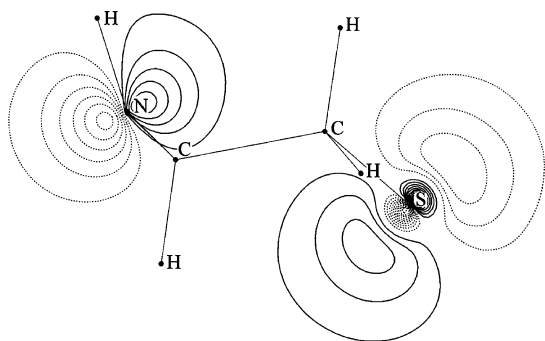


Figure 4. Calculated spin density distribution for the radical cation of thiomorpholine in the N-H bond-sulfur atom plane.

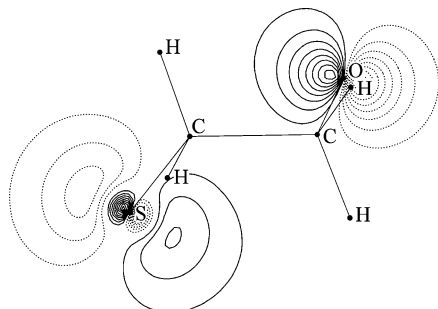


Figure 5. Spin density distribution for the radical cation of thioxane in the S-O plane, which is parallel to the C-C bonds.

Regarding the relative stability of different conformers, the radical cation of thiomorpholine shows the same tendency as piperazine and morpholine cations; that is, the “chair” conformation (Figure 4) is definitely the most stable. Spin populations at sulfur and nitrogen atoms in “chair” conformation are almost equal (0.407 and 0.421, respectively). Thus, two pairs of hydrogen atoms in the β -position with respect to the nitrogen atom give coupling constants of 0.92 and 0.77 mT, respectively. Two protons in the β -position to sulfur exhibit a hyperfine coupling constant of 0.82 mT, whereas the second pair of the corresponding protons shows very small hyperfine coupling (see Table 2).

The “boat” conformers of the radical cation with axial and equatorial positions of N-H bond position lie respectively 8.7 and 7.7 kcal/mol above the “chair” conformation. Similar to the cases of piperazine and morpholine, these conformers would yield very large proton hyperfine coupling constants (according to our calculations, from 1.5–3.5 up to 6.1 mT).

Thioxane. Again, the most favorable calculated conformation of a neutral molecule is “chair”. “Twist” and “boat” conformers were found to have much higher energy (at least, by 5 kcal/mol).

The most favorable calculated conformation of the radical cation is “chair” with the spin population concentrated mainly at the P_z orbital of sulfur atom (the spin density at oxygen atom is much lower (approximately by a factor of 3; see Figure 5). According to calculations, one could expect the coupling constants of 1.42 mT for two hydrogen atoms in the β -position to S, whereas two protons occupying the β -position with respect to the oxygen atom should have coupling constants of 0.93 mT. The calculated hyperfine coupling constants for the other four protons are much smaller (below 0.4 mT).

The radical cation of thioxane in a distorted “boat” conformation is definitely less stable (by 8.32 kcal/mol). In comparison with the “chair” conformer, the spin population at the sulfur atom becomes higher, whereas the spin population at oxygen

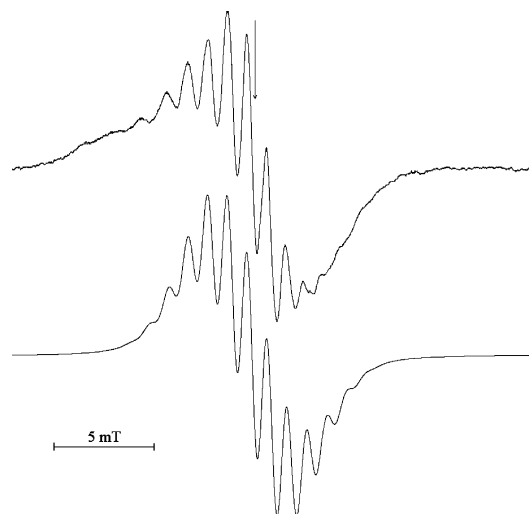


Figure 6. EPR spectrum of an irradiated frozen solution of piperazine (0.3%) in Freon-11 recorded at 155 K (top) and simulated spectrum of piperazine radical cation. The simulation was made using HFC constants given in Table 2 with a Lorentzian line width of 0.62 mT. The ENDOR field position is marked with an arrow.

atom becomes lower. In this case, one could expect the biggest proton coupling constant, as large as 4.7 mT.

EPR and ENDOR Spectra

Piperazine. The EPR spectra of the piperazine radical cation in Freon-11 recorded at 77 K reveal a multiplet pattern of a large number of nearly equidistant lines with the observed splitting of ca. 0.9–1 mT, which is qualitatively similar to those reported for the dimethylpiperazine cation.¹¹ Warming the samples to 155 K results in somewhat better resolution (Figure 6; note that all the spectral changes between 77 and 155 K are reversible). The main reason for the observed temperature dependence should be dynamic averaging of anisotropic couplings for nitrogen nuclei and the α -protons (N-H protons), whereas the effect of temperature on the β -proton couplings appears to be negligible because of large barriers for ring inversion (“chair”–“chair” or “chair”–“boat” interconversion) in six-member heterocycles.¹⁹ It is worthwhile noting that the dynamics of EPR spectra associated with averaging of nitrogen hyperfine coupling anisotropy was observed experimentally and analyzed in detail for the morpholin-1-yl radical in a Freon-113 matrix in the temperature range 77–135 K.¹² On the basis of the data obtained for this radical,¹² one should expect nearly complete averaging of anisotropic couplings for related six-member heterocyclic species at temperatures above 135 K, which justifies using isotropic approximation.

Unfortunately, we were unable to obtain a sufficiently good ENDOR spectrum for the piperazine radical cation. However, in this case, the EPR spectra are well resolved, so the interpretation appears to be rather straightforward.

As typical for nitrogen-centered radical cations, g anisotropy is small,²⁰ and it can be neglected in the first approximation. We applied an isotropic simulation to fit the EPR spectrum obtained at the highest attainable temperature (155 K). The symmetry constraints were held on fitting; that is, it was assumed that the radical cation possessed two sets of equivalent β -protons (four protons in each set) and two equivalent N-H protons. The best-fit hyperfine coupling constants (expressed in millitesla) are given in Table 2. The difference between experimental and simulated EPR spectra at the spectral “wings” may be attributed to presence of broad signals from matrix radicals.

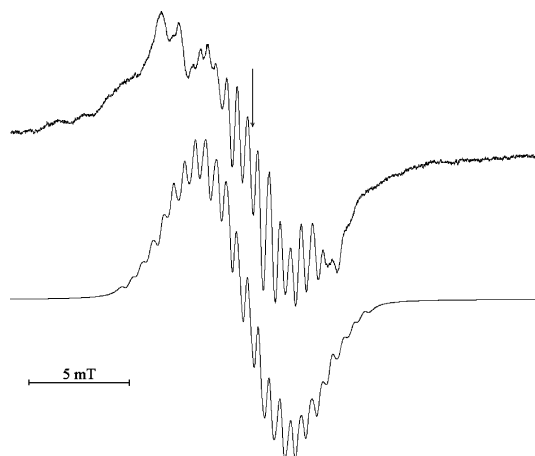


Figure 7. EPR spectrum of irradiated frozen solution of morpholine (0.3%) in Freon-11 recorded at 155 K (top) and simulated spectrum of morpholine radical cation. The simulation was made using HFC constants given in Table 2 and a Lorentzian line width of 0.27 mT. The ENDOR field position is marked with an arrow.

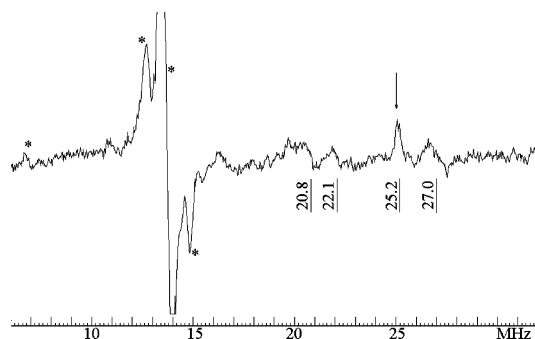


Figure 8. ENDOR spectrum of an irradiated frozen solution of morpholine in Freon-11 measured at 110 K. Asterisks show the signals from the matrix species. The arrow shows a sharp line that is tentatively assigned to the perpendicular component of the N-H proton HFC tensor.

Morpholine. The EPR spectrum obtained at 77 K is poorly resolved, with the smallest observable splitting of ca. 1.0 mT. Meanwhile, the spectra recorded at 115–155 K show distinct splittings of about 0.5 mT (see Figure 7). Similar to the case of piperazine, all the spectral changes with temperature are reversible, which gives no indications of any thermal-induced chemical transformations. Again, we attribute the spectral changes mainly to averaging of anisotropic couplings.

The ENDOR spectra taken at 110 K (Figure 8) show signals at 20.8, 22.1, 25.2, and, 27.0 MHz. With an assumption that we observe only a high-frequency line of each pair (see above), these values may be converted to the proton hyperfine splittings of 0.45, 0.54, 0.77, and 0.90 mT, consistent with the observed EPR spectra (an alternative interpretation of these ENDOR signals leads to the values 2.52, 2.61, 2.69, and 2.83 mT, which are definitely too large and can be ruled out). One should note that, in general, the morpholine radical cation has five sets of protons, which could give ENDOR features (four pairs of β -protons and the N-H proton). Regarding the line shape, one may note that sharp feature at 25.2 MHz marked with an arrow (corresponding to the HFC constant of 0.77 mT) is significantly different from all the other lines. For this reason, we suggest tentatively that this sharp line may arise from the perpendicular component of the N-H proton HFC tensor (assuming nearly axial symmetry for this tensor at 110 K). In this case, three other observed features may be assigned

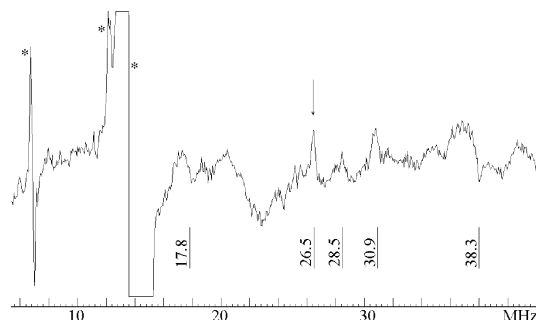


Figure 9. ENDOR spectrum of irradiated frozen solution of thiomorpholine in Freon-11 measured at 70 K. Asterisks show the signals from the matrix species. The arrow shows a sharp line that is tentatively assigned to perpendicular component of the N-H proton HFC tensor.

to β -protons (broadening of the corresponding ENDOR signals can be explained by small residual anisotropy of β -proton couplings).

Assignment of the observed ENDOR signals to specific β -protons can be made from comparison with the calculated data (Table 2). Indeed, three of four calculated coupling constants (0.44, 0.53, and 0.83 mT) are in very good agreement with the ENDOR data (0.45, 0.54, and 0.90 mT, respectively). Meanwhile, one calculated HFC constant (1.48 mT) differs much from all the values derived from ENDOR. Most probably, the corresponding feature is lost in ENDOR for some reason, which is not fully clear. An attempt was made to fit the experimental EPR spectrum recorded at 155 K using an isotropic simulation, where three coupling constants were fixed in accordance to the data derived from ENDOR measurements, whereas the other constants (for one set of β -protons, N-H proton, and ^{14}N nucleus) were fitted using the calculated values as starting points. The result of fitting is shown in Figure 7, and the best-fit values are given in Table 2. One can see that simulation reproduces the central part of the experimental EPR spectrum reasonably well, whereas the spectral wings (especially, in the low-field region) show significant deviations because of the presence of broad, apparently anisotropic signal. The latter signal may result from matrix radical. Indeed, adding a broad doublet signal with the splitting of ca. 7 mT (reasonable for Freon radical) results in much better agreement between the theoretical and experimental spectra. In addition, we cannot fully exclude certain admixture of morpholin-1-yl radicals, which could be formed in morpholine clusters occurring even at high dilution.¹²

Thiomorpholine. The EPR spectra obtained for thiomorpholine radical cation show relatively small reversible variations within the temperature range of 30–150 K. In this case, the line width of the components is considerably larger (ca 0.9 mT), and the smallest observable splitting is as large as ca. 1.3 mT.

It should be noted that we did not observe prominent anisotropy of the \mathbf{g} -tensor of the thiomorpholine radical cation (either at 110 K or at lower temperatures). This means that, in terms of \mathbf{g} -tensor properties, the thiomorpholine radical cation is close to nitrogen-centered species rather than to sulfur-centered radicals. Qualitatively, this is in accord with the calculated spin density distribution; however, detailed interpretation of this fact requires further experimental and theoretical work.

The ENDOR spectra taken at 70 K reveal a sharp signal at 26.5 MHz (Figure 9). Similar to the line at 25.2 MHz in the case of morpholine, it may be assigned tentatively to a perpendicular feature of the HFC tensor for the N-H proton. Other features in the spectrum measured at 70 K are rather broad and



Figure 10. EPR spectrum of irradiated frozen solution of thiomorpholine (0.3%) in Freon-11 recorded at 110 K (top) and simulated spectrum of thiomorpholine radical cation. The simulation was made using HFC constants given in Table 2 and a Lorentzian line width of 0.63 mT. The ENDOR field position is marked with an arrow.

very weak (the spectra recorded at higher temperatures were of even poor quality). Nevertheless, we may assign tentatively four signals appearing at 17.8, 28.5, 30.9, and 38.3 MHz. Conversion of these ENDOR frequencies into proton hyperfine couplings yields the HFC constants 0.25, 1.01, 1.19, and 1.71 mT (an alternative assignment of these constants is 2.87, 3.05, 3.22, and 3.75 mT, and these values are too large to be considered). All these features may be ascribed to four sets (pairs) of β -protons. The three latter values look quite reasonable in view of the average splitting of 1.3 mT in the EPR spectrum, whereas the smallest splitting (0.25 mT) cannot be resolved in EPR.

An isotropic simulation of the EPR spectrum (Figure 10) was made using the values derived from ENDOR for β -protons and fitting the coupling constants for the ^{14}N and N-H proton (see Table 2). The simulation describes the central part of the spectrum reasonably well, whereas the low-field wing is not well fitted. We attribute the difference to neglect of anisotropy and contribution from matrix species.

Comparison of experimental and calculated values reveals significant underestimation of some proton couplings, especially for the largest coupling constant (Table 2), so the assignment of the experimental coupling constants to specific protons may be considered only as tentative.

Thioxane. The EPR spectrum of irradiated thioxane in a Freon-11 matrix shows a complex, strongly asymmetrical pattern (Figure 11). A remarkable g anisotropy and relatively large effective g -value (ca. 2.015, as estimated from the position of the spectrum center) are characteristic for the S-centered radicals.⁹ The low-field part of the spectrum shows better resolution, revealing distinct structure with the observed splitting of ca. 0.7–0.8 mT. It is worthwhile noting that the EPR spectra of the thioxane radical cation do not reveal any pronounced temperature dependence in the range 110–150 K. This observation can be understood by taking into account that the reversible temperature dependence of the spectra of the radical cations of nitrogen containing heterocycles was explained by motional averaging of anisotropic hyperfine couplings (see above). Meanwhile, g anisotropy in the thioxane radical cation is not completely averaged even at relatively high temperatures.

The ENDOR spectrum recorded at 110 K shows signals at 15.5, 18.3, 22.4, and 25.2 MHz (Figure 12). All of these signals exhibit "anisotropic" line shape indicating relatively small dipole contribution characteristic of β -proton coupling. Each line may

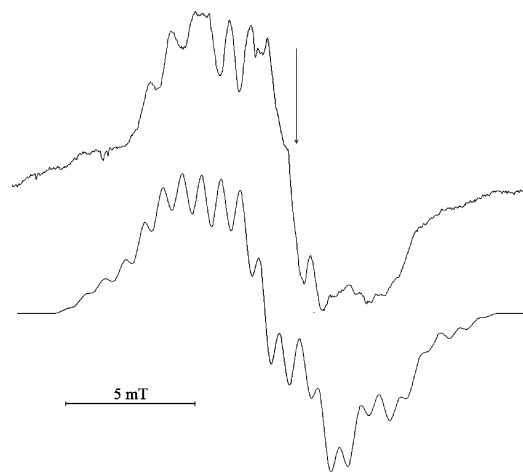


Figure 11. EPR spectrum of irradiated frozen solution of thioxane (0.3%) in Freon-11 recorded at 110 K (top) and simulated spectrum of thioxane radical cation. The simulation was made using HFC constants given in Table 2 and a Lorentzian line width of 0.44 mT. The ENDOR field position is marked with an arrow.

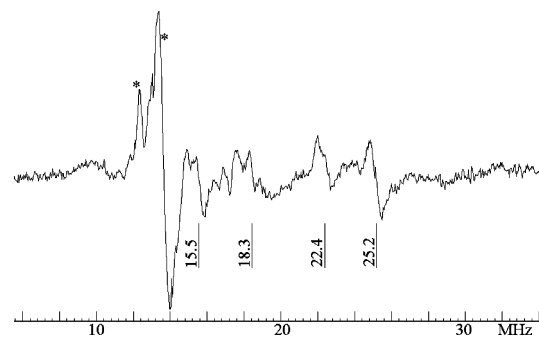


Figure 12. ENDOR spectrum of irradiated frozen solution of thioxane in Freon-11 measured at 110 K. Asterisks show the signals from matrix species.

be converted into hyperfine coupling constants in two ways. Thus, the observed ENDOR signals may correspond to the coupling constants of 0.08 or 2.12 mT (15.5 MHz), 0.28 or 2.32 mT (18.3 MHz), 0.56 or 2.61 mT (22.4 MHz), and 0.77 or 2.81 mT (25.2 MHz). The observed splitting of 0.7–0.8 mT in the EPR spectrum is consistent with the coupling constant of 0.78 mT. Meanwhile, the relatively large total spread of the EPR spectrum makes us suggest that the two former ENDOR lines should correspond to larger coupling constants, i.e., 2.13 and 2.34 mT rather than 0.08 and 0.28 mT. This interpretation is also favored by the following consideration. In the case of coupling constants of 0.08 and 0.28 mT, the observed lines are the high-frequency components of the corresponding pairs in the ENDOR spectra. For such values of the coupling constants the pairing line of approximately the same intensity should appear at 13 and 10.2 MHz; however, this is not the case. On the other hand, the suggested interpretation (2.13 and 2.34 mT) implies that we observe the low-frequency signals. In this case, the corresponding high-frequency components could be observed at ca. 44.8 and 47.1 MHz, which is out of the scanning range of our ENDOR spectra. Note that these coupling constants are approximately 3 times higher than the smaller coupling constant, which may account for occurrence of multiple lines separated by 0.7–0.8 mT. In this case, the residual coupling constant corresponding to the ENDOR line at 18.3 MHz should be 0.57 mT, because the alternative value of 2.63 mT is too large and results in overestimation of the total spread of the EPR spectrum. Therefore, we may assign the hyperfine coupling values of 0.57,

TABLE 3: Calculated Spin Population Distribution between Two Heteroatoms

radical cation	spin population on N atom	spin population on S atom	spin population on O atom
morpholine (N, O)	0.522		0.198
piperazine (N, N)	2 × 0.377		
thiomorpholine (N, S)	0.421	0.407	
thioxane (S, O)		0.617	0.199

0.78, 2.13, and 2.34 mT to four sets of β -protons in the thioxane radical cation. A set of anisotropic powder simulations was made using isotropic hyperfine constants derived from ENDOR (without any fitting) and varying only the \mathbf{g} -tensor. The best fit for the spectrum recorded at 110 K was obtained for the following tensor: $g_1 = 2.0257$; $g_2 = 2.0147$; $g_3 = 2.0047$. We should note that, strictly speaking, these values cannot be treated as the principal values of the rigid \mathbf{g} -tensor, because partial motional averaging may occur under the experimental conditions used. Meanwhile, the value of $g_{\text{iso}} = 2.015$ looks quite typical for S-centered radicals. The agreement between simulated and experimental spectra in this approximation is rather rough. Meanwhile, even this simulation reproduces the total spectrum spread and small splittings, especially in the low-field part. The difference in the high-field region may be attributed to the obvious reasons (oversimplifications in simulation and presence of matrix radicals) and also to possible contribution from dimer radical cation (a broad singlet with lower g -value, which dominates at high concentrations of thioxane).

Discussion

The results of our calculations show that the systems under consideration have 72–83% of total spin density located on heteroatoms. Delocalization to the carbon atoms of the ring is relatively more important for piperazine and morpholine and less significant for thiomorpholine and thioxane. The calculated distribution of spin population (sp) between two heteroatoms in heterocyclic radical cations is given in Table 3. In general, one can see the following trend for the systems with two different heteroatoms: $\text{sp(N)} \approx \text{sp(S)} \ll \text{sp(O)}$. In the cases of oxygen containing heterocycles, the oxygen atom bears relatively low spin population (ca. 20% for both morpholine and thioxane). Thus, it is quite understandable that we do not observe large HFC constants for protons in β -position in respect to oxygen (unlike the case of ether radical cations, where spin is mainly located at the oxygen atom). The spin population of nitrogen and, in particular, sulfur atoms may be substantially higher (up to 62% of total spin population for S in thioxane radical cation). However, it does not result in large coupling with the corresponding β -protons via hyperconjugation mechanism because of more diffuse nature of outer sulfur atomic orbitals.

Generally speaking, a common feature of all the radical cations under study is concerned with relatively small hyperfine couplings for β -protons (in contrast with cyclic radical cations with single heteroatom or two heteroatoms in positions 1 and 3). From a qualitative point of view, this feature is reproduced by the DFT calculations. In all the cases, the calculated structures correspond to the “chair” conformers, whereas the “twist” and “boat” conformers are essentially less stable. Furthermore, the latter structures normally show in calculations very large, nonrealistic proton coupling constants. Thus, there is no reason to assume intramolecular σ^* -bonding in the “boat”-shaped structures to explain the observed small couplings, as was suggested tentatively in early works.^{6,11}

Quantitative comparison of experimental and calculational results is given in Table 2. As follows from this table, in the cases of piperazine and morpholine, the agreement between experimental hyperfine coupling constants for β -protons and results of the DFT calculations is reasonable (typically, within 10–30%). In the case of thiomorpholine, two calculated HFC constants for β -protons are in reasonable agreement with experiment, whereas the smallest and largest constants are underestimated approximately by the factor of 2. As to the smallest one, we do not pay much attention to this difference, because this coupling is undetectable in EPR, and assignment of the corresponding ENDOR line is tentative. Also, this small coupling may be affected strongly by a slight deviation in conformation, e.g., because of the matrix effect. Meanwhile, poor agreement between calculated and experimental values for the largest HFC constant appears to reflect some problem of DFT calculations.

The largest discrepancy between experiment and calculations is observed for thioxane radical cations: all the calculated hyperfine coupling constants are considerably underestimated, and it cannot be corrected by simple scaling. It is clear that the calculated HFC constants fail to reproduce the total spread of the experimental spectrum. Thus, the calculated geometry of the thioxane radical cation may differ from the experimental one. To get some information about the experimental conformation of this radical cation, we can apply the so-called “ $\cos^2 \theta$ rule”,

$$a_{\beta}^{\text{H}} \approx B\rho \cos^2 \theta$$

for the HFC constants at β -protons of p-electron radicals, where B is a constant characteristic of specific p-atom associated with radical site, ρ is the spin population at the p_z orbital, and θ is the dihedral angle between the p_z orbital and C–H $_{\beta}$ bond. This rule is known to work well for the O-centered radical cations of linear and cyclic ethers and S-centered radical cations of the corresponding sulfides, if we assume that spin population is concerned with the p_z orbital of heteroatoms, $B(\text{O}) \approx 9.0$ mT and $B(\text{S}) \approx 4.2$ mT, respectively.^{1,6,9} The application of this law to the radical cations with two heteroatoms studied in this work is not so straightforward, because the spin density is partially delocalized to the carbon atoms of the ring (in other words, the treatment of C–H protons as “pure β -protons” is not rigorous). Nevertheless, in the case of thioxane, a major part of the spin population is associated with S and O atoms (see above), and one can try to estimate the dihedral angles from simple consideration by taking into account only hyperconjugation of C–H protons with the p_z orbitals of heteroatoms. Following the qualitative conclusion from calculations, we may assign tentatively the largest and the smallest coupling constants (2.34 and 0.57 mT) to two pairs of protons at C atoms adjacent to S. In this case, the ratio of constants (ca. 4) clearly suggests $\theta_1 \approx 0^\circ$, $\theta_2 \approx 60^\circ$, and $B(\text{S}) \rho(\text{S}) \approx 2.34$ mT (the corresponding projection is shown in Figure 13 a). Analogous consideration for the other two pairs of protons with the HFC constants of 2.13 and 0.78 mT (β -protons in respect to O) results in $\theta_1 \approx 7^\circ$, $\theta_2 \approx 53^\circ$, and $B(\text{O}) \rho(\text{O}) \approx 2.16$ mT (Figure 13b). According to this consideration, the steric configurations of all the carbon atoms in the thioxane radical cation are rather similar; they correspond to a distorted chair conformation. Using $B(\text{S})$ and $B(\text{O})$ values given above, one can obtain rough estimates of “experimental” spin populations at p_z orbitals: $\rho(\text{S}) \approx 0.56$ and $\rho(\text{O}) \approx 0.24$, which are in reasonable agreement with the calculated values (0.62 and 0.20, respectively). On the other

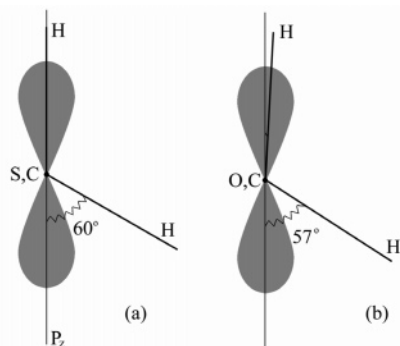


Figure 13. Relative position of C–H $_{\beta}$ bonds and the p_z orbital of the heteroatom, namely sulfur (a) and oxygen (b), derived from ENDOR constants and the “ $\cos^2 \theta$ rule”.

hand, the calculated dihedral angles show significant deviations from those derived from the “ $\cos^2 \theta$ rule”.

Conclusions

Calculational and experimental data obtained in this work reveal that the radical cations of six-member heterocycles with two heteroatoms in 1,4-positions adopt a chair (or distorted chair) conformation with spin density distributed mainly between the p -orbitals of heteroatoms. Formation of a three-electron intramolecular σ^* -bond in a boat conformation appears to be a unique feature of the 1,4-dithiane radical cation, which does not occur in heterocycles containing N and O atoms. In general, the DFT calculations give quite reasonable predictions of magnetic resonance parameters for heterocycles with N and O atoms (note that the hyperfine couplings in known 1,4-dioxane radical cations are also reproduced well by the calculation method used in this work). The discrepancy observed for S containing species (in particular, for thioxane) may be explained either by some problems of theory at this level or by the unusually strong matrix effect on the experimental conformation of the radical cation. More work is necessary to clarify this issue.

It is worthwhile noting that a nonsymmetrical spin and charge distribution in the radical cations of heterocycles with different heteroatoms may result in specific site-selective reactivity of

these species. The study of chemical properties of radical cations considered in this paper and related heterocyclic species is in progress now.

Acknowledgment. We acknowledge the help of H. Gustafsson in the ENDOR experiments. This work was supported by INTAS (project no. 2000-0093) and Russian Foundation for Basic Research (project no. 03-03-32717).

References and Notes

- (1) Symons, M. C. R. *Chem. Soc. Rev.* **1984**, *13*, 393.
- (2) *Radical Ionic Systems Properties in Condensed Phases*; Lund, A., Shiotani, M., Eds.; Kluwer: Dordrecht, The Netherlands, 1991.
- (3) Shiotani, M. *Magn. Reson. Rev.* **1987**, *12*, 333.
- (4) Feldman, V. I. In *EPR of Free Radicals in Solids. Trends in Methods and Applications*; Lund, A., Shiotani, M., Eds.; Kluwer: Dordrecht, The Netherlands, 2003.
- (5) Snow, L. D.; Wang, J. T.; Williams, F. J. *Am. Chem. Soc.* **1982**, *104*, 2062.
- (6) Symons, M. C. R.; Wren, B. W. *J. Chem. Soc., Perkin Trans. 2* **1984**, 511.
- (7) Belevskii, V. N.; Khvan, O. In; Belopushkin, S. I.; Feldman, V. I. *Dokl. Akad. Nauk SSSR* **1985**, *281*, 869.
- (8) Naumov, S.; Janovsky, I.; Knolle, W.; Mehnert, R. *Phys. Chem. Chem. Phys.* **2003**, *5*, 3133.
- (9) Ramakrishna Rao, D. N.; Symons, M. C. R.; Wren, B. W. *J. Chem. Soc., Perkin Trans. 2* **1984**, 1681.
- (10) Bonazzola, L.; Michaut, J. P.; Roncin, J. *Can. J. Chem.* **1988**, *66*, 3050.
- (11) Eastland, G. W.; Ramakrishna Rao, D. N.; Symons, M. C. R. *J. Chem. Soc., Perkin Trans. 2* **1984**, 1551.
- (12) Antzutkin, O. N.; Benetis, N. P.; Lindgren, M.; Lund, A. *Chem. Phys.* **1993**, *169*, 195.
- (13) Erickson, R. In *Electron Magnetic Resonance of Free Radicals. Theoretical and Experimental EPR, ENDOR and ESEEM Studies of Radicals in Single Crystal and Disordered Solids*. Linköping Studies in Science and Technology. Dissertation No. 391. Linköping, 1995.
- (14) Whiffen, D. H. *Mol. Phys.* **1966**, *10*, 595.
- (15) Perdew, J. P.; Burke, K.; Ernzerhof, M. *Phys. Rev. Lett.* **1996**, *77*, 3865.
- (16) Laikov, D. N. *Chem. Phys. Lett.* **1997**, *281*, 151.
- (17) Laikov, D. N. Ph.D. (Phys. Math.) Thesis, Moscow State University, Moscow, 2000 (in Russian).
- (18) Eriksson, L. A.; Malkin, V. G.; Malkina, O. L.; Salahub, D. R. *J. Chem. Phys.* **1993**, *99*, 9756.
- (19) Sjöqvist, L.; Lindgren, M.; Lund, A. *Chem. Phys. Lett.* **1989**, *156*, 323.
- (20) Eastland, G. W.; Ramakrishna Rao, D. N.; Symons, M. C. R. *J. Chem. Soc., Perkin Trans. 2* **1984**, 1551.